



Formation of spikes and bubbles in the linear phase of Rayleigh-Taylor instability in elastic-plastic media

A. R. Piriz **Instituto de Investigaciones Energéticas (INEI), E.T.S.I.I., and CYTEMA, Universidad de Castilla-La Mancha, 13071 Ciudad Real, Spain*S. A. Piriz *Instituto de Investigaciones Energéticas (INEI), E.I.I.A., and CYTEMA, Universidad de Castilla-La Mancha, 45071 Toledo, Spain*

N. A. Tahir

GSI Helmholtzzentrum für Schwerionenforschung Darmstadt, Planckstrasse 1, 64291 Darmstadt, Germany

(Received 12 November 2022; accepted 3 March 2023; published 20 March 2023)

The generation of spikes and bubbles, a typical characteristic of the nonlinear regime in the Rayleigh-Taylor instability, is found to occur as well during the linear regime in an elastic-plastic solid medium caused, however, by a very different mechanism. This singular feature originates in the differential loads at different locations of the interface, which makes that the transition from the elastic to the plastic regime takes place at different times, thus producing an asymmetric growth of peaks and valleys that rapidly evolves in exponentially growing spikes, while bubbles can also grow exponentially at a lower rate.

DOI: [10.1103/PhysRevE.107.035105](https://doi.org/10.1103/PhysRevE.107.035105)

I. INTRODUCTION

The Rayleigh-Taylor instability (RTI) in accelerated solids with elastic-plastic (EP) mechanical properties [1–10] is a central issue in the design of the LAPLAS (Laboratory Planetary Science) experiment planned at the GSI Helmholtzzentrum Darmstadt (Germany) in the framework of the high-energy-density (HED) international collaborations developed around the heavy-ion accelerator FAIR (Facility for Ion and Antiproton Research) [11–18]. It is also relevant to physical phenomena present in many different scenarios, ranging from applications to experiments on HED material sciences [19–22] to geophysics and astrophysics [22–26].

The nonlinear character of the constitutive properties of EP media introduces a number of peculiarities into the evolution of RTI that makes this physical process very interesting in its own right. In fact, it is the only known case of RTI in which the stability conditions are determined by the amplitude of the perturbation as well as by its wavelength. In addition, in the stable cases, it shows the existence of two kinds of stable regimes, one in the elastic phase of the instability and another one in the plastic phase. As it was shown in Ref. [1], the latter makes plastic flow a necessary but not sufficient condition for instability.

In this work we report another unique feature of RTI in EP media that is also a direct consequence of their specific mechanical properties and that gives rise to the formation of spikes and bubbles when the instability evolution is still in the linear phase. In the general case, this kind of asymmetric evolution of peaks and valleys is proper of the nonlinear evolution

of the instability, and arises as a consequence of the lateral forces acting on the protuberances of the medium that tend to squeeze the peaks and to widen the valleys, thus leading to the formation of spikes and bubbles, respectively [27]. Just for clarity, let us mention that we are calling peaks and valleys protuberances and depressions, respectively, of the solid media, which is the opposite to the topographic convention determined by the orientation of the gravity (Fig. 1).

In the present case of RTI in EP media, the asymmetric growth of peaks and valleys is the direct result of the differential transition from the elastic to the plastic regime in different parts of the interface that are submitted to different deformations. This issue has been overlooked so far in all the previous works, in which the main interest was centered on the time evolution of the instability. The plastic phase of the instability was treated by following the Drucker observation that a sinusoidal perturbation on the interface should be considered like a set of bumps of height twice the amplitude of the perturbation, which applies a loading force on the bottom level (the valleys level). Then, the total force was estimated by averaging it over half a wavelength [28,29]. Therefore, the effect of this differential deformation at different points on the interface was missed.

Here we will take into account the spatial variation of the loading on the interface at different positions, in order to study the asymmetric evolution of peaks and valleys, which leads to the singular feature of formation of spikes and bubbles during the linear evolution of RTI. For this it is sufficient to restrict ourselves to the simplest configuration consisting in a semi-infinite EP medium supported against gravity by the pressure of a massless fluid (Fig. 1). This situation was already considered in Ref. [1] for studying the stability boundaries in the irrotational approximation, and it also constitutes a

*roberto.piriz@uclm.es

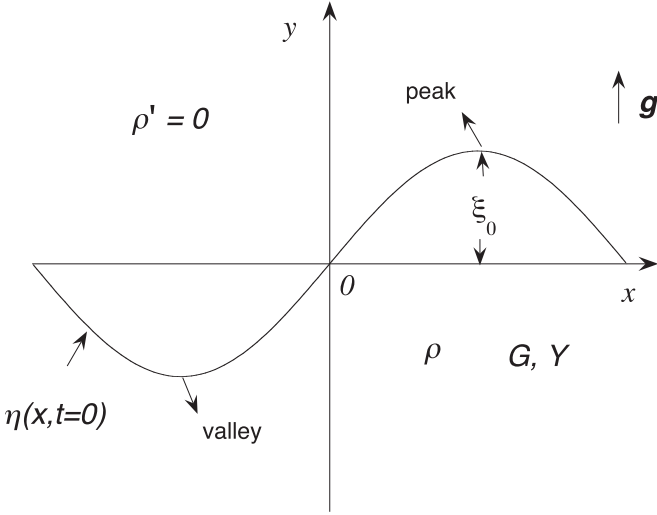


FIG. 1. Schematic of the perturbed interface between an elastic-plastic ($y < 0$) medium and a massless ideal fluid ($y > 0$).

limiting case of the configuration studied in Ref. [7] when a very thick layer is considered ($kh \gg 1$, $k = 2\pi/\lambda$ is the perturbation wave number and h is the layer thickness), and the Atwood number A_T is taken equal to one.

II. LINEAR ANALYSIS

We consider the situation schematically represented in Fig. 1 of a very thick (semi-infinite) solid medium of density ρ with elastic-plastic constitutive properties that will be described as an ideal elastic-plastic material characterized by an elastic shear modulus G and a yield strength Y . The solid lies on the top of a massless ideal fluid under the action of a constant gravity $\mathbf{g} = g\mathbf{e}_y = -\nabla\varphi$ (\mathbf{e}_y is the unitary vector in the vertical direction and φ is the gravitational potential).

For the analysis we follow the procedure described in Refs. [7,8] that we will briefly review here in order to obtain the equation of motion of the interface during the elastic and plastic phases of the RTI evolution. We start with the conservation equations for mass and momentum for a continuous medium:

$$\frac{d\rho}{dt} + \rho \frac{\partial v_i}{\partial x_i} = 0, \quad (1)$$

$$\rho \frac{dv_i}{dt} = -\frac{\partial p}{\partial x_i} + \rho g_i + \frac{\partial \sigma_{ik}}{\partial x_k}, \quad (2)$$

where i, k denote the space coordinates x, y, z in the index notation for Cartesian tensors, and for the vertical coordinate $i \equiv y$, we have $g_i \equiv g = -\partial\varphi/\partial y$, while $g_i = 0$ for $i \neq y$. In addition v_i , ρ , and p are the corresponding components of the velocity, the density, and the pressure, respectively, and σ_{ik} is the deviatoric part of the stress tensor $\Sigma_{ik} = -p\delta_{ik} + \sigma_{ik}$ of the medium (δ_{ik} is the Kronecker δ).

On the other hand, the material derivative of any magnitude M in Eqs. (1) and (2) is

$$\frac{dM}{dt} = \frac{\partial M}{\partial t} + v_i \frac{\partial M}{\partial x_i}. \quad (3)$$

Then, we linearize Eqs. (1) and (2) as usual, so that a magnitude M is written as $M = M_0 + \delta M$, where M_0 is the equilibrium value and $\delta M \ll M_0$ is the perturbation. As a result, for incompressible perturbations ($\delta\rho = 0$) we get:

$$\frac{\partial(\delta v_i)}{\partial x_i} = 0, \quad (4)$$

$$\rho \frac{\partial(\delta v_i)}{\partial t} = -\frac{\partial(\delta p + \rho\delta\varphi)}{\partial x_i} + \frac{\partial S_{ik}}{\partial x_k}, \quad (5)$$

where we have called S_{ik} the perturbation $\delta\sigma_{ik}$ of the deviatoric part of the stress tensor. In addition, for the elastic-plastic medium we adopt the nonlinear constitutive equations expressing a perfectly elastic Hookean behavior for the smaller strains, and a behavior like a perfectly rigid plastic when the stress overcomes the elastic limit Y [1,1–10,30,33]. Then, for the elastic phase, we have:

$$\frac{\partial S_{ik}}{\partial t} = 2G\dot{e}_{ik} \quad e_{ik} = \frac{1}{2} \left[\frac{\partial \eta_i}{\partial x_k} + \frac{\partial \eta_k}{\partial x_i} \right], \quad (6)$$

where upper dots denote time derivative, and e_{ik} is the perturbation of the strain tensor. In addition, η_i are the components of the perturbed displacement vector $\boldsymbol{\eta}$ so that $\dot{\eta}_i = \delta v_i$.

On the other hand, for the plastic phase we can write [1–10,30,33]:

$$S_{ik} = \sqrt{\frac{2}{3}} \frac{\dot{e}_{ik}}{\|\dot{e}_{ik}\|} Y_{\text{eff}}, \quad (7)$$

where $Y_{\text{eff}} = \beta Y$ ($\beta > 1$) is an effective value of the yield strength that takes into account that, in order to satisfy the usual von Mises criterion (corresponding to $\beta = 1$) at a distance of the order of k^{-1} from the interface ($y = 0$), a larger deformation must be achieved at the interface. In fact, as it was discussed in Refs. [7–10] the transition from the regime in which RTI is controlled by the elastic properties, to the one in which it is controlled by the plastic ones, requires that the region above the interface, within a distance of k^{-1} , overcomes the phase of contained plastic flow such as it is expressed by the von Mises criterion [28,29]. Since deformation decays with the distance from the interface, it will be larger at the interface than at $y \sim -k^{-1}$. This feature can be taken into account by assuming an effective yield strength $Y_{\text{eff}} > Y$ in Eq. (7). Anyway, this is just a quantitative consideration that has no qualitative consequence on the present problem. With the previous considerations, we will obtain the equations of the interface separately for the elastic and for the plastic phases as in Refs. [7–10].

A. Elastic phase

As it was described in previous works, we will use here the Helmholtz decomposition for the displacement field [7–10]:

$$\boldsymbol{\eta} = \nabla\phi + \nabla \times (\boldsymbol{\psi}\mathbf{e}_z), \quad (8)$$

where ϕ and $\boldsymbol{\psi} = \psi\mathbf{e}_z$ are, respectively, the Lamé scalar and vector potentials functions. By introducing the previous

equation into Eqs. (4) and (5), we get the following equations that determine the potential functions [3–10]:

$$\nabla^2 \phi = 0, \quad (9)$$

$$\nabla \left(\frac{\partial^2 \phi}{\partial t^2} + \frac{\delta p}{\rho} + \delta \varphi \right) + \nabla \times \left[\left(\frac{\partial^2 \psi}{\partial t^2} - \frac{G}{\rho} \nabla^2 \psi \right) \mathbf{e}_z \right] = 0, \quad (10)$$

where $\delta \varphi = -\rho g \eta_y$. As it is well known, Eq. (10) can be split into two equations by taking advantage of the extra degree of freedom introduced by the vector potential. Then, it turns out [31,32]:

$$\rho \frac{\partial^2 \phi}{\partial t^2} + \delta p - \rho g \eta_y = 0, \quad (11)$$

$$\rho \frac{\partial^2 \psi}{\partial t^2} = G \nabla^2 \psi. \quad (12)$$

By considering two-dimensional perturbations and solving Eq. (11) and (12), we obtain the following expressions for the potential functions in the solid medium during the elastic phase:

$$\phi(x, y, t) = a(t) e^{ky} \sin kx, \quad (13)$$

$$\psi(x, y, t) = b(t) e^{qy} \cos kx, \quad (14)$$

where

$$q(k) = \sqrt{k^2 + \frac{\gamma_{en}^2 \rho}{G}}, \quad (15)$$

and a, b , are functions of time such that

$$a(t) \propto b(t) \propto \sum_n Q_n e^{\gamma_{en} t}, \quad (16)$$

where Q_n are constants, and γ_{en} are the asymptotic growth rates resulting from all the possible solutions of the dispersion relation that will be determined, together with the time functions a and b , by the boundary conditions on the interface. These boundary conditions require the continuity of the vertical velocity and of the normal and tangential stresses through the interface. Then, for the vertical velocity at $y = 0$, we have:

$$\delta v_y(0) = \dot{\eta}_v(x, t), \quad (17)$$

where have defined η_v as follows:

$$\eta_v(x, t) = \eta_y(x, t, y = 0), \quad (18)$$

and $v = e$ or p denotes the elastic or the plastic regimes, respectively.

Then, for the elastic phase we are now considering, we have:

$$\eta_e(x, t) = \xi_e(t) \sin kx, \quad (19)$$

where $\xi_e(t)$ represents the maximum instantaneous amplitude of the perturbation. Then, Eq. (17) yields:

$$\dot{\xi}_e(x, t) = k(\dot{a} + \dot{b}), \quad (20)$$

For the tangential stresses at $y = 0$, we have $S_{xy}(0) = 0$ and we get:

$$\dot{b} = -\frac{2k^2}{q^2 + k^2} \dot{a}, \quad (21)$$

In addition, for the normal stresses, we have at $y = 0$:

$$-\delta p(0) + S_{yy}(0) = 0, \quad (22)$$

where

$$S_{yy}(0) = 2kG(ka + qb + C_0) \sin kx, \quad (23)$$

with C_0 being an integration constant resulting from the time integration of Eq. (6). Then, Eq. (22) reads:

$$-\rho \ddot{a} + \rho g \xi_e = 2kG(ka + qb + C_0). \quad (24)$$

Thus, by noticing that

$$\ddot{a} = \frac{\ddot{\xi}_e}{k} + \frac{\ddot{\xi}_e}{k} \frac{2k^2 G}{\rho \gamma_{en}^2}, \quad (25)$$

and using Eqs. (20) and (21), the previous equations yield the equation of motion of the interface during the elastic phase:

$$\rho \frac{\ddot{\xi}_e}{k} + S_{ye} = \rho g \xi_e, \quad (26)$$

where

$$S_{ye} = 2kG \left[\frac{\ddot{\xi}_e - \ddot{\xi}_0}{\gamma_{en}^2} + \frac{q-k}{q+k} (\xi_e - \xi_0) \right], \quad (27)$$

with $\xi_0 = \xi_e(t=0)$ and $\ddot{\xi}_0 = \ddot{\xi}_e(t=0)$. In writing Eqs. (26) and (27) we have taken into account that stress-free initial conditions requires that at $t = 0$ it must be $\ddot{\xi}_0 = k g \xi_0$. Besides, these equations must be solved with the following initial conditions:

$$\xi_e(t=0) = \xi_0 \quad \dot{\xi}_e(t=0) = 0. \quad (28)$$

It may be worth to notice that Eqs. (26) and (27) are equally satisfied by the local amplitude $\eta_e(x, t)$ given by Eq. (19), and this feature will be used later when considering the spatial shape of the perturbation.

As it was shown in Ref. [5], the previous equations yield the following asymptotic dispersion relation:

$$\gamma_{en}^2 - kg = \frac{4k^2 G}{\rho} \left[-1 + \frac{kG}{\gamma_{en}^2 \rho} \left(\sqrt{k^2 + \frac{\gamma_{en}^2 \rho}{G}} - k \right) \right]. \quad (29)$$

A very good approximation of the growth rate can be obtained in the irrotational limit, which results for $k^2 \gg \gamma_{en}^2 \rho / G$ [1,5,33]:

$$\gamma_{en}^2 \approx kg - \frac{2k^2 G}{\rho}. \quad (30)$$

Certainly, this simple expression can be obtained from the very beginning, by adopting the irrotational approximation, from Eqs. (13), (17), and (22) [1,5,33]. It will allow us to keep the theory completely analytic without missing any essential physics, and it will be used hereafter. As it is well known this growth rate presents a cutoff wave number $k_c = \rho g / 2G$ beyond which the interface is elastically stable and oscillates with a frequency ω such that $\omega^2 = -\gamma_{en}^2$ [5,33,34].

Therefore, the solution of Eqs. (26) and (27) with the boundary conditions given by Eq. (28), read:

$$\frac{\xi_e}{\xi_0} = 1 + \frac{kg}{\gamma_{en}^2} (\cosh \gamma_{en} t - 1) \quad \text{for } k \leq k_c. \quad (31)$$

$$\frac{\xi_e}{\xi_0} = 1 + \frac{kg}{\omega^2} (1 - \cos \omega t) \quad \text{for } k \geq k_c. \quad (32)$$

Besides, we notice that since $\ddot{\xi}_e - \ddot{\xi}_0 = \gamma_{en}^2 (\xi_e - \xi_0)$, and that in the irrotational approximation it is $q \approx k$, Eq. (27) yields:

$$S_{ye} \approx 2kG(\xi_e - \xi_0). \quad (33)$$

B. Plastic phase

As in previous works, we consider here classical plasticity, so that the displacement field will be irrotational [7–10,35]. Then, the vector potential is a constant that can be taken as $\psi = 0$, and the scalar potential ϕ is given by Eq. (13). On the other hand, as it was first noticed by Drucker, the initial sinusoidal perturbation on the interface, must be considered as a succession of protuberances of high $2\xi_0$, so that the total loading on the bottom level that leads to plastic flow, is determined by the whole material contained between the peaks and the valleys (bottom of the valleys in the plastic phase is at $y = -\xi_p(t)$ at the time t) [28,29]. Therefore, from Eq. (22), the equation of motion during the plastic phase is

$$\frac{\rho}{k} \ddot{\eta}_p + S_{yp} = \rho g \eta_p, \quad (34)$$

where η_p must be referred to the bottom level of the valleys:

$$\eta_p(x, t) = \xi_p(t)(1 + \sin kx). \quad (35)$$

On the other hand, S_{yp} is given by Eq. (7), with $\|\dot{e}_{ik}\|^2 = \dot{e}_{xx}^2 + \dot{e}_{yy}^2 + 2\dot{e}_{xy}^2$. Since the tangential stress is $S_{xy} = 0$, and incompressibility imposes $\dot{e}_{xx} = -\dot{e}_{yy}$, it turns out $\|\dot{e}_{ik}\|^2 = 2\dot{e}_{yy}^2$. Therefore, we get

$$S_{yp} = \frac{Y_{\text{eff}}}{\sqrt{3}}. \quad (36)$$

It is worth to notice that S_{yp} does not depend on the x coordinate and, therefore, the spatial dependence of the deformation $\eta_p(x, t)$ cannot be dropped from the equation of motion given by Eq. (34), such as it was done in Eq. (26) for the elastic phase.

Thus, the general solution of Eq. (34) is

$$\eta_p(t) = \frac{Y_{\text{eff}}}{\sqrt{3}\rho g} + K_1' e^{\gamma_p t} + K_2' e^{-\gamma_p t}; \quad \gamma_p = \sqrt{k}g, \quad (37)$$

where the constants $K_{1,2}'$ have to be determined from the matching conditions between the solutions for the elastic and for the plastic regimes at the transition time t_T . For this, first we need to refer also the elastic solution to the valleys bottom level by redefining $\eta_e(x, t)$ in Eq. (19) as follows:

$$\eta_e(x, t) = \xi_e(t)(1 + \sin kx), \quad (38)$$

which, of course, also satisfies Eq. (26). Then, the matching conditions read:

$$\eta_e(x, t_T) = \eta_p(x, t_T) \quad \dot{\eta}_e(x, t_T) = \dot{\eta}_p(x, t_T), \quad (39)$$

C. Stability and EP transition boundaries

As discussed in previous works, in order to determine the region of stability, it is sufficient to consider the elastic stable solutions given by Eqs. (32) and (38), together with the solution for the plastic phase given in Eq. (37) and then to impose the conditions for marginal stability, which have to be satisfied when the perturbation amplitude η achieves an absolute maximum at a certain time $t_M \geq t_T$ [1,7–10]:

$$\dot{\eta}(t_M) = 0; \quad \ddot{\eta}(t_M) = 0; \quad (t_M \geq t_T). \quad (40)$$

For this, it is convenient to introduce first the following dimensionless magnitudes:

$$z = \frac{\eta}{\xi_0}; \quad T = t\sqrt{k_0 g}; \quad \Omega = i\sigma = \frac{\omega}{\sqrt{k_0 g}}; \quad k_0 = \frac{\rho g}{G}. \quad (41)$$

Then, Eqs. (32), (37), and (38) yield

$$z_e(X, T) = \left[1 + \frac{\sigma_p^2}{\Omega^2} (1 - \cos \Omega T) \right] (1 + \sin X); \quad T \leq T_T, \quad (42)$$

$$z_p(T) = \frac{1}{\xi^*} + K_1 e^{\sigma_p T} + K_2 e^{-\sigma_p T}; \quad T \geq T_T, \quad (43)$$

where

$$\xi^* = \frac{\sqrt{3}\rho g \xi_0}{Y_{\text{eff}}}; \quad \sigma_p = \sqrt{\kappa}; \quad X = kx; \quad \kappa = \frac{k}{k_0}, \quad (44)$$

and T_T is the dimensionless transition time, when the matching conditions of Eq. (39) must be satisfied for a given fixed value of X . On the other hand, from Eqs. (26), (33), (34), and (36), we see that at the time T_T for which $\eta(T_T) = \eta_T = \xi_T(1 + \sin kx)$, the following relationship is found:

$$2kG(\xi_T - \xi_0)(1 + \sin kx) \approx \frac{Y_{\text{eff}}}{\sqrt{3}}. \quad (45)$$

Or, in dimensionless form:

$$(z_T - 1)(1 + \sin X) \approx \frac{\lambda^*}{\xi^*}; \quad \lambda^* = \frac{\rho g \lambda}{4\pi G}, \quad (46)$$

which, from Eq. (32), can also be written as follows:

$$\frac{\sigma_p^2}{\Omega^2} (1 - \cos \Omega T_T)(1 + \sin X) \approx \frac{\lambda^*}{\xi^*}. \quad (47)$$

As we will see later, the previous equation, together with Eq. (31) or Eq. (32) evaluated in $t = t_T$, gives the instant T_T when the transition from the elastic to the plastic regime takes place for a given fixed position X on the interface. Alternatively, for a given time T , it also determines the position X_T that separates the parts of the interface that are still evolving in the elastic regime from those that are already in the plastic regime. That is, the peak of the perturbation ($X = \pi/2$) is the first to make the transition to the plastic regime and, as time evolves, the transition point moves towards the valleys ($X = -\pi/2$), which at the bottom remain always in the RTI regime controlled by the elastic properties, unless they achieve first the stable plastic regime, as we will see later. In other words, Eq. (46) shows that the elastic strain necessary to achieve the elastic limit is determined essentially by Y_{eff} , but the amplitude necessary to achieve such a strain is different for

every position X and, therefore, it will be achieved at different times.

The constants $K_{1,2}$ in Eq. (43) are determined from the matching conditions at $T = T_T$ given in Eq. (39):

$$K_1 = \frac{A+B}{2}; \quad K_2 = \frac{A-B}{2}, \quad (48)$$

where

$$A = \left[1 + \frac{\sigma_p^2}{\Omega^2} (1 - \cos \Omega T_T) \right] (1 + \sin X) - \frac{1}{\xi^*}, \quad (49)$$

$$B = \frac{\sigma_p}{\Omega} (1 + \sin X) \sin \Omega T_T. \quad (50)$$

Besides, in order to satisfy the conditions for marginal stability of Eq. (40), we can put $K_2 = 0$ at $T = T_T$ [8–10], and the following relationship turns out:

$$\begin{aligned} & \left[1 + \frac{\sigma_p^2}{\Omega^2} (1 - \cos \Omega T_T) \right] (1 + \sin X) - \frac{1}{\xi^*} \\ &= \frac{\sigma_p}{\Omega} (1 + \sin X) \sin \Omega T_T. \end{aligned} \quad (51)$$

By eliminating ΩT_T from Eqs. (47) and (51), we get the following equation for $\eta^* = \xi^*(1 + \sin X)$ giving the stability boundaries:

$$(\eta^*)^2 - 2\eta^* + H - 1 + \left(\frac{H\Omega}{\sigma_p} \right)^2 = 0; \quad H = \frac{q+k}{2k} \lambda^*, \quad (52)$$

As it was already mentioned, for the present purpose it is sufficient to adopt the irrotational approximation, which allows us to keep the analysis completely analytic without missing any fundamental physics. Then, for $\kappa^2 \gg \Omega^2$ it is

$$q \approx k; \quad \Omega \approx \sqrt{2\kappa^2 - \kappa}, \quad (53)$$

and with $\kappa = 1/(2\lambda^*)$, Eq. (52) becomes [1]:

$$\eta^* \approx 1 - \sqrt{\lambda^*}. \quad (54)$$

This expression yields the condition for marginal stability at any fixed position X on the interface, and we have represented it in Fig. 2. Of course, the absolute condition for stability of the interface is determined by the less stringent case corresponding to the peak at $X = \pi/2$.

In the same figure we show the boundary for the EP transition, which corresponds to the situation when plastic flow occurs just at the time of maximum amplitude of the elastic oscillation in the stable regime. In the irrotational approximation it reads [1]:

$$\eta_{EP}^* \approx \frac{1}{2}(1 - \lambda^*). \quad (55)$$

Figure 2 shows that the perturbations grow unstably for $\lambda^* > 1$ and for any perturbation amplitude, and also for $\lambda^* < 1$ for amplitudes $\eta > 1 - \sqrt{\lambda^*}$. In both cases, a part of the unstable interface will evolve in the plastic regime while the rest may do it in the elastic regime. This differential growth at different parts of the interface produces the progressive deformation of the initial sinusoidal profile of the interface leading to the formation of linear spikes and bubbles.

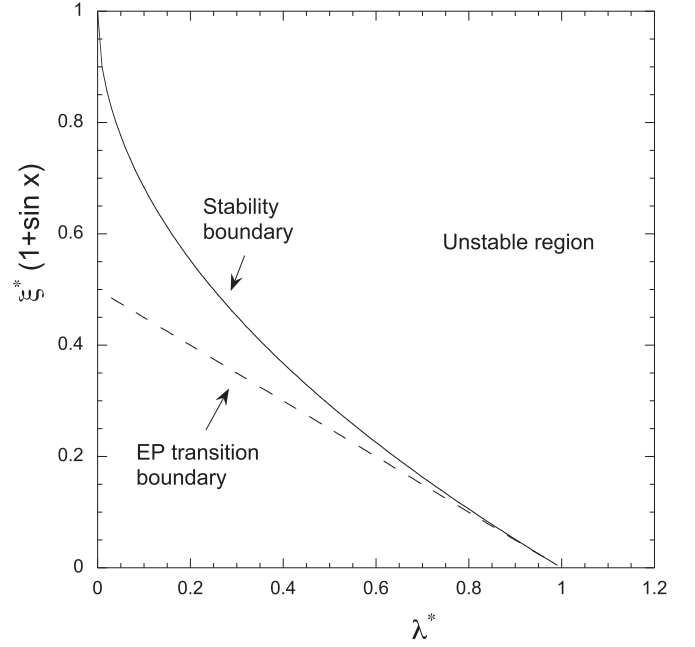


FIG. 2. Boundaries for stability (full line) and for the elastic-plastic transition (dotted line).

III. SPIKES AND BUBBLES FORMATION

A. $\lambda^* > 1$

In this regime the interface is always unstable, evolving elastically at early times at a given position X and, then, continuing plastically at later times. Let us first to consider the shape of the interface at a fixed time T . From Eqs. (31), (38), (43), and Eqs. (48)–(51) we obtain:

$$z(X, T \leq T_T) = \left[1 + \frac{\sigma_p^2}{\sigma_e^2} (\cosh \sigma_e T - 1) \right] (1 + \sin X). \quad (56)$$

$$\begin{aligned} z(X, T \geq T_T) &= \frac{1}{\xi^*} + A(X) \cosh[\sigma_p(T - T_T)] \\ &\quad + B(X) \sinh[\sigma_p(T - T_T)], \end{aligned} \quad (57)$$

where $\sigma_e^2 = -\Omega^2$ is given by Eq. (53) and, from Eqs. (46), (49), and (50), we write:

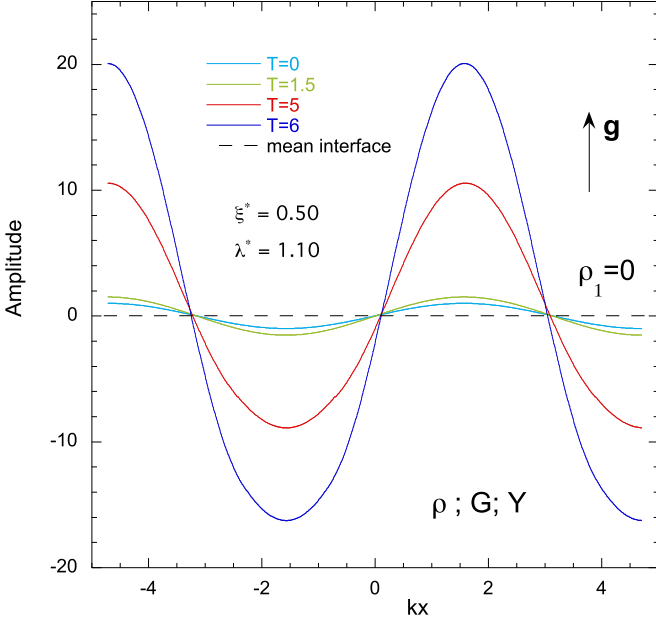
$$A(X) = 1 + \sin X + \frac{\lambda^* - 1}{\xi^*}. \quad (58)$$

$$B(X) = \frac{\sigma_p}{\sigma_e} \sqrt{\left(1 + \sin X + \frac{\lambda^* \sigma_e^2}{\xi^* \sigma_p^2} \right)^2 - (1 + \sin X)^2}. \quad (59)$$

$$T_T(X) = \frac{1}{\sigma_e} \operatorname{arcosh} \left[1 + \frac{\lambda^* \sigma_e^2}{\xi^* \sigma_p^2} \frac{1}{1 + \sin X} \right]. \quad (60)$$

In order to represent the interface profile we need to refer the amplitude back again to the mean interface. For this we need to invoke the conservation of the total mass, which requires that, at any given time, spikes and bubbles contain an equal amount of mass.

Thus, the interface profile is shown in Fig. 3 for several different times, and for the particular case of $\lambda^* = 1.10$ and $\xi^* = 0.5$. At $T = 0$ the interface is perfectly sinusoidal. At


FIG. 3. Interface profile at different times for $\lambda^* > 1$.

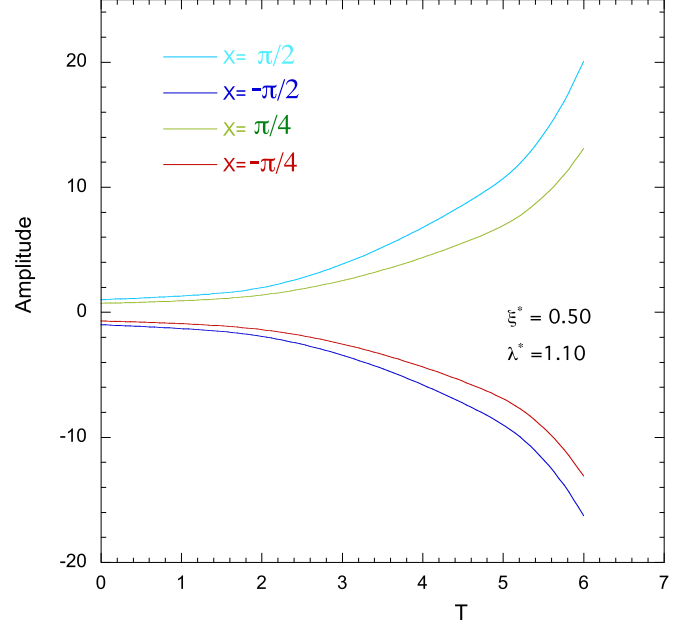
relatively short times like $T = 1.5$, the perturbation is growing elastically and only a small part near the peak is growing in the plastic regime. Thus, it still has a practically sinusoidal shape. As the time advances, a progressively larger part of the peak grows plastically while the rest, mainly in the valley region, continues evolving in the elastic regime and, therefore it grows at a smaller rate. As a consequence, at $T = 5$ a clear asymmetry is observed between the peaks and the valleys due to the different elastic and plastic growth rates, giving origin to the formation of spikes and bubbles, respectively. This is already very evident at $T = 6$ although at this time RTI will be still in linear regime.

For instance, in the case considered in Refs. [7,9,10,12–18] of a strongly accelerated tungsten media ($Y = 2.2 \text{ GPa}$, $G = 160 \text{ GPa}$), and taking $\beta = 3$, we have $z_{\text{peak}} \approx 20$ for $T = 6$ ($\xi^* = 0.5$, $\lambda^* = 1.1$). Then,

$$k\xi_{\text{peak}} = \frac{\beta}{2\sqrt{3}} \frac{Y}{G} \frac{\xi^*}{\lambda^*} z_{\text{peak}} \approx 0.11. \quad (61)$$

That is, RTI is still in the linear regime even at this rather long time.

We can now consider the time evolution of the interface, which we have represented in Fig. 4 and shows the perturbation amplitude as a function of time for several different locations of the interface. Namely, at the peaks ($X = \pi/2$), at the valleys ($X = -\pi/2$), and at two intermediate positions ($X = \pi/4$ and $X = -\pi/4$). As it can be seen, at early times, when the perturbation grows in the elastic regime, the growth is symmetrical for peaks and valleys. The symmetry endures for a longer time at the intermediate locations, like $X = \pm\pi/4$. Then, at sufficiently long times, the perturbation starts to grow in the plastic regime in the peaks, so that they grow faster than the valleys, which are still in the elastic regime. This behavior is similar for larger values of λ^* but the


FIG. 4. Amplitude of the perturbation as a function of time for different locations on the interface for $\lambda^* > 1$.

time required for the appearance of the asymmetry becomes progressively longer.

B. $\lambda^* < 1$

This case presents some differences because, as it is shown in Fig. 2, for relatively small amplitudes the interface is stable. Therefore, some parts close to the peaks are growing in the unstable plastic regime, while regions close to the bottom of the valleys remain in the stable elastic or plastic regimes, thus slowing down the growth of the entire bubble.

The shape of the interface for a fixed time T is now given by Eqs. (32), (38), (43), and Eqs. (48)–(51), which yield:

$$z(X, T \leq T_0) = \left[1 + \frac{\sigma_p^2}{\sigma_e^2} (1 - \cos \Omega T) \right] (1 + \sin X). \quad (62)$$

$$z(X, T \geq T_0) = \frac{1}{\xi^*} + A(X) \cosh[\sigma_p(T - T_0)] + B'(X) \sinh[\sigma_p(T - T_0)], \quad (63)$$

where $A(x)$ is still given by Eq. (58) and

$$B'(X) = \frac{\sigma_p}{\sigma_e} \sqrt{(1 + \sin X)^2 - \left(1 + \sin X + \frac{\lambda^* \sigma_e^2}{\xi^* \sigma_p^2} \right)^2}. \quad (64)$$

In addition, the time T_0 is the lesser between the time $T_m = \pi/\Omega$ when the elastic oscillation achieves the maximum, and the time T'_T :

$$T'_T(X) = \frac{1}{\Omega} \arccos \left[1 - \frac{\lambda^* \Omega^2}{\xi^* \sigma_p^2} \frac{1}{1 + \sin X} \right]. \quad (65)$$

If the transition occurs at $T'_T < T_m$, then $T_0 = T'_T$, and the instability goes first from the elastic stable regime to the

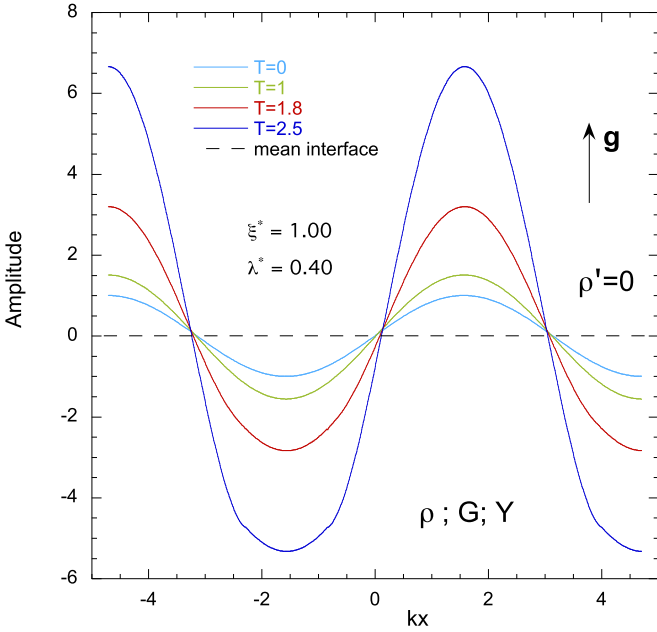


FIG. 5. Interface profile at different times for $\lambda^* < 1$.

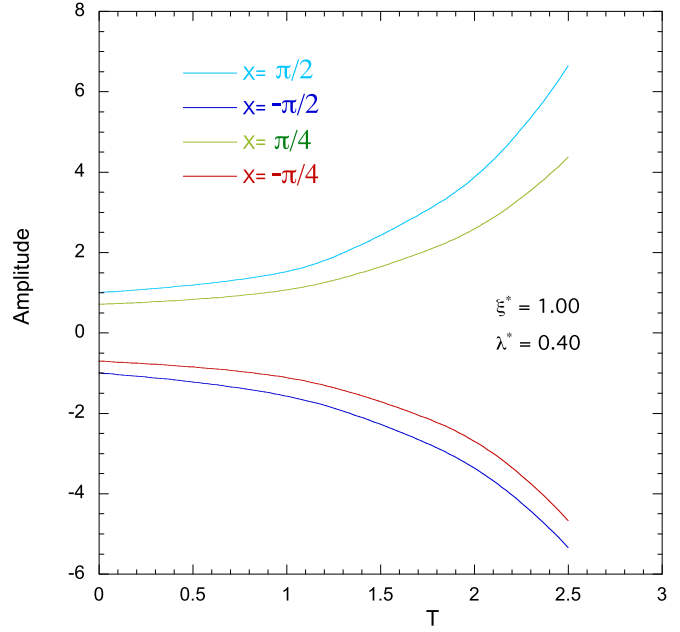


FIG. 6. Amplitude of the perturbation as a function of time for different locations on the interface for $\lambda^* < 1$.

plastic stable regime. Instead, when $T'_T \geq T_m$, it is $T_0 = T_m$, and it goes directly to the plastic unstable regime.

In Fig. 5 we show the resulting shape of the interface at different times. At $T = 0$ the interface is sinusoidal and, as time progresses, the amplitude increases by following the initial stage of an elastic oscillation ($T = 1$) [1]. Then, at later times, it achieves the plastic regime in which the parts of the interface close to the valleys remain plastically stable, while those close to the peaks have already reached the unstable plastic regime. This gives rise to an asymmetric evolution that makes the peaks to progressively develop in spikes and the valleys in bubbles ($T = 1.8$ and $T = 2.5$).

This behavior is also appreciated in Fig. 6 where we have represented the time evolution of the interface at different locations. Once again, we can see that, at early times, peaks ($X = \pi/2$) and valleys ($X = -\pi/2$) grow symmetrically. But once the peaks enter in the plastic regime, they grow exponentially while the bottom of the valleys remain stable in the plastic regime thus making the bubbles to grow to a slower rate.

For intermediate positions, as for instance $X = \pm\pi/4$, the behavior is quite similar but with a slower growth ($X = \pi/4$), or at practically the same growth since the regions close to the bottom of the valleys remain elastically stable ($X = -\pi/4$).

IV. CONCLUDING REMARKS

We have shown the existence of another unique feature of RTI in EP media, which leads to the formation of spikes and bubbles in the linear regime of growth of the instability. This behavior is a consequence of the nonlinear character of the constitutive properties that makes the medium to behave as a Hookean elastic material for the smallest deformations, and as a plastic material when it overcomes a certain limit. This is because the required deformation for the transition from

the elastic to the plastic regime is determined by the yield strength, being a material property that is invariant all over the interface. While the deformation, instead, changes at different points of the interface. Therefore, the plastic flow threshold in each different location is achieved at different times, thus giving place to a differential deformation of the surface that leads to the creation of spikes and bubbles. However, differently from the nonlinear case, the present linear spikes have an exponential growth.

The mechanism described here is very different from the one present in the standard nonlinear regime of the RTI, which is caused essentially by the rise of lateral forces on the peaks and valleys that tend to squeeze the former and to expand the latter [27]. Actually, one should expect that when RTI in EP media enters in the nonlinear regime, both mechanisms will be present, thus affecting the late evolution of the interface and probably accelerating the formation of the spikes. On the other hand, it can be speculated that a similar process may also take place in a similar phenomenon like the Richtmyer-Meshkov instability in EP media, which is currently studied in the framework of jets generation [36–40].

Finally, we want to point out that the change in the shape of a sinusoidal perturbation during the RTI evolution in a solid was already predicted by Drucker in Ref. [28] based on heuristic arguments, although the concept was not further analyzed.

ACKNOWLEDGMENTS

This work has been partially supported by the Ministerio de Economía y Competitividad of Spain (Grant No. PID2021-125550OB-I00), and by the BMBF of Germany.

- [1] A. R. Piriz, J. J. López Cela, and N. A. Tahir, *Phys. Rev. E* **80**, 046305 (2009).
- [2] S. A. Piriz, A. R. Piriz, and N. A. Tahir, *Phys. Rev. E* **95**, 053108 (2017).
- [3] S. A. Piriz, A. R. Piriz, and N. A. Tahir, *Phys. Rev. E* **96**, 063115 (2017).
- [4] S. A. Piriz, A. R. Piriz, and N. A. Tahir, *Phys. Rev. E* **97**, 043106 (2018).
- [5] S. A. Piriz, A. R. Piriz, and N. A. Tahir, *J. Fluid Mech.* **867**, 1012 (2019).
- [6] S. A. Piriz, A. R. Piriz, and N. A. Tahir, *Phys. Fluids* **30**, 111703 (2018).
- [7] A. R. Piriz, S. A. Piriz, and N. A. Tahir, *Phys. Rev. E* **100**, 063104 (2019).
- [8] S. A. Piriz, A. R. Piriz, N. A. Tahir, S. Richter, and M. Bestehorn, *Phys. Rev. E* **103**, 023105 (2021).
- [9] A. R. Piriz, S. A. Piriz, and N. A. Tahir, *Phys. Rev. E* **104**, 035102 (2021).
- [10] A. R. Piriz, S. A. Piriz, and N. A. Tahir, *Phys. Rev. E* **106**, 015109 (2022).
- [11] J. F. Barnes, P. J. Blewett, R. G. McQueen, K. A. Meyer, and D. Venable, *J. Appl. Phys.* **45**, 727 (1974).
- [12] N. A. Tahir, I. V. Lomonosov, B. Borm, A. R. Piriz, P. Neumayer, A. Shutov, V. Bagnoud, and S. A. Piriz, *Contrib. Plasma Phys.* **57**, 493 (2017).
- [13] N. A. Tahir, P. Neumayer, I. V. Lomonosov, A. Shutov, V. Bagnoud, A. R. Piriz, S. A. Piriz, and C. Deutsch, *Phys. Rev. E* **101**, 023202 (2020).
- [14] N. A. Tahir, I. V. Lomonosov, B. Borm, A. R. Piriz, A. Shutov, P. Neumayer, V. Bagnoud, and S. A. Piriz, *Astrophys. J. Suppl. Series* **232**, 1 (2017).
- [15] N. A. Tahir, A. Shutov, I. V. Lomonosov, A. R. Piriz, P. Neumayer, V. Bagnoud, and S. A. Piriz, *Astrophys. J. Suppl. Series* **238**, 27 (2018).
- [16] N. A. Tahir, P. Neumayer, A. Shutov, A. R. Piriz, I. V. Lomonosov, V. Bagnoud, S. A. Piriz, and C. Deutsch, *Contrib. Plasma Phys.* **59**, e201800143 (2019).
- [17] N. A. Tahir, A. Shutov, A. R. Piriz, P. Neumayer, I. V. Lomonosov, V. Bagnoud, and S. A. Piriz, *Contrib. Plasma Phys.* **59**, e201800135 (2019).
- [18] N. A. Tahir, A. Shutov, P. Neumayer, V. Bagnoud, A. R. Piriz, I. V. Lomonosov, and S. A. Piriz, *Phys. Plasmas* **28**, 032712 (2021).
- [19] D. H. Kalantar, B. A. Remington, J. D. Colvin, K. O. Mikaelian, S. V. Weber, L. G. Wiley, J. S. Wark, A. Loveridge, A. M. Allen, A. A. Hauer, and M. A. Meyers, *Phys. Plasmas* **7**, 1999 (2000).
- [20] J. D. Colvin, M. Legend, B. A. Remington, G. Shurtz, and S. V. Weber, *J. Appl. Phys.* **93**, 5287 (2003).
- [21] B. A. Remington, P. Allen, E. M. Bringa, J. Hawreliak, D. Ho, K. T. Lorenz, H. Lorenzana, J. M. McNaney, M. A. Meyers, S. W. Pollaine, K. Rosolankova, B. Sadik, M. S. Schneider, D. Swift, J. Wark, and B. Yaakobi, *Mater. Sci. Technol.* **22**, 474 (2006).
- [22] H-S. Park, K. T. Lorenz, R. M. Cavallo, S. M. Pollaine, S. T. Prisbrey, R. E. Rudd, R. C. Becker, J. V. Bernier, and B. A. Remington, *Phys. Rev. Lett.* **104**, 135504 (2010).
- [23] G. H. Houseman and P. Molnar, *Geophys. J. Int.* **128**, 125 (1997).
- [24] E. B. Burov and P. Molnar, *Earth Planet. Sci. Lett.* **275**, 370 (2008).
- [25] W. Gorczyk, B. Hobbs, K. Gessner, and T. Gerya, *Gondwana Research* **24**, 838 (2013).
- [26] O. Blaes, R. Blandford, and P. Madau, *Astrophys. J.* **363**, 612 (1990).
- [27] E. Ott, *Phys. Rev. Lett.* **29**, 1429 (1972).
- [28] D. C. Drucker, in *Mechanics Today*, edited by S. Nemat-Nasser (Pergamon, Oxford, 1980), Vol. 5, p. 37.
- [29] D. C. Drucker, *Ing. arch* **49**, 361 (1980).
- [30] A. R. Piriz, J. J. López Cela, N. A. Tahir, and D. H. Hoffmann, *Phys. Rev. E* **78**, 056401 (2008).
- [31] A. C. Eringen and E. S. Suhubi, *Elastodynamics. Vol. II: Linear Theory* (Academic Press, New York, 1975).
- [32] K. S. Thorne and R. G. Blandford, *Modern Classical Physics* (Princeton University Press, Princeton, 2017), Chap. 12.
- [33] A. R. Piriz, J. J. López Cela, O. D. Cortazar, N. A. Tahir, and D. H. Hoffmann, *Phys. Rev. E* **72**, 056313 (2005).
- [34] G. Terrones, *Phys. Rev. E* **71**, 036306 (2005).
- [35] M. E. Gurtin and L. Anand, *J. Mech. Phys. Solids* **53**, 1624 (2005).
- [36] G. Dimonte, G. Terrones, F. J. Cherne, T. C. Germann, V. Dupont, K. Kadau, W. T. Buttler, D. M. Oro, C. Morris, and D. L. Preston, *Phys. Rev. Lett.* **107**, 264502 (2011).
- [37] W. T. Buttler, D. M. Oro, D. L. Preston, K. O. Mikaelian, F. J. Cherne, R. S. Hixson, F. G. Mariam, C. Morris, J. B. Stone, G. Terrones, and D. Tupa, *J. Fluid Mech.* **703**, 60 (2012).
- [38] B. J. Jensen, F. J. Cherne, M. B. Prime, K. Fezzaa, A. J. Iverson, C. A. Carlson, J. D. Yeager, K. J. Ramos, D. E. Hooks, J. C. Cooley, and G. Dimonte, *J. Appl. Phys.* **118**, 195903 (2015).
- [39] M. B. Prime, W. T. Buttler, S. J. Fensin, D. R. Jones, J. L. Brown, R. S. King, R. Manzanares, D. T. Martinez, J. I. Martinez, J. R. Payton, and D. W. Schmidt, *Phys. Rev. E* **100**, 053002 (2019).
- [40] D. M. Sterbentz, C. F. Jekel, D. A. White, and J. L. Belof, *Phys. Fluids* **34**, 082109 (2022).